Measurement 160 (2020) 107851

Contents lists available at ScienceDirect

Measurement

journal homepage: www.elsevier.com/locate/measurement

Uncertainty of mass flow measurement using centric and eccentric orifice for Reynolds number in the range 10,000 ≤ *Re* ≤ 20,000

Anna Golijanek-Jędrzejczyk [a,*], Andrzej Mrowiec [b], Robert Hanus [c], Marcin Zych [d], Dariusz Świsulski [a]

[a] Gdańsk University of Technology, Faculty of Electrical and Control Engineering, 80-233 Gdańsk, Poland
[b] The President Stanislaw Wojciechowski State University of Applied Sciences in Kalisz, Polytechnic Faculty, 62-800 Kalisz, Poland
[c] Rzeszów University of Technology, Faculty of Electrical and Computer Engineering, 35-959 Rzeszów, Poland
[d] AGH University of Science and Technology, Faculty of Geology, Geophysics and Environmental Protection, 30-059 Kraków, Poland

ARTICLE INFO

Article history:
Received 13 November 2019
Received in revised form 9 March 2020
Accepted 11 April 2020
Available online 18 April 2020

Keywords:
Flow measurement
Mass flow
Orifice
Uncertainty analysis
Monte Carlo

ABSTRACT

The article analyses the impact of the Reynolds number on the estimated uncertainty of the mass flow rate measurement using an orifice plate. The objects of the research were two types of orifices: centric (ISA) and eccentric, with the diameter ratio $\beta = 0.5$. Studies were performed by Monte Carlo simulation and experiments for Reynolds numbers in the range $10{,}000 \leq Re \leq 20{,}000$. The obtained results have shown that for both orifice types, the results obtained from the experiments and from the Monte Carlo simulation are similar. The nature of changes in the expanded uncertainty of the flow measurement is very similar for each type. For the both types of orifices, the value of the expanded uncertainty of the flow measurement increases linearly with the increasing Reynolds number.

1. Introduction

Despite the existence of different methods of flow rate measurement, orifices are the most commonly used type of flowmeters in the oil, gas, nuclear and conventional energy, and chemical industries [1,2]. This type of flowmeter is characterized by high utility regardless of whether the medium in the installation is liquid or gas [3–5]. Such a widespread use of orifices comes from the simplicity of the design and installation, lack of moving parts, and the resulting high reliability [1,2,6]. Another advantage of this method is its low cost of implementation and operation. In combination with other measuring methods, described for example in the articles [7–11], the orifice-based measurement can be used to control multiphase flows. Orifice flowmeters also have disadvantages, the main ones being high pressure drop and high sensitivity to the orifice inlet profile [12]. This impact is limited by satisfying the condition of large straight pipe length before the flowmeter [1]. However, despite these drawbacks, this type of flowmeters is estimated to account for around 40% of market share [6].

Due to such a widespread use of orifices, it is very important to estimate the accuracy of flow measurements making use of them [13–15]. It is obvious that such estimates must be made both when a new type of orifice is used [16–19] (e.g. centric, cylindrical flange-tapped orifice), and when performing interlaboratory comparisons between accredited laboratories [20,21].

It should also be borne in mind that according to current metrological recommendations of GUM [22,23], every correctly performed measurement requires that its result be supplemented with a qualitative parameter characterizing this measurement, i.e. with the value of error or uncertainty. That is why it is extremely important to determine the uncertainty of flow measurement regardless of the type of fluid flowing through the orifice: from fuel oil [24], through water [12,25] to saline water [26].

This article describes the results of the authors' work on a project regarding water flow measurements using various orifices and estimating the accuracy of measurements [12]. The aim of the work presented in this article was to check the influence of the Reynolds number on the estimated measurement uncertainty for two types of orifices: centric (ISA) and eccentric. Preliminary results only for the centric orifice have been partially published in [15]. In this article, the authors present the results of experimental and simulation studies for the centric and eccentric orifice. The aim was also to check whether the nature of changes in the uncertainty of flow measurement depends on the type of orifice used in the installation. The authors have not found any results of this type of research in the available literature. The article is a continuation of the work presented in [12], where the influence of individual physical quantities on the final value of uncertainty of flow

* Corresponding author.
E-mail address: annjedrz@pg.edu.pl (A. Golijanek-Jędrzejczyk).

https://doi.org/10.1016/j.measurement.2020.107851
0263-2241/

measurement was considered for one set value of Reynolds number. Extending the present analysis to different *Re* values is justified by the increasing flow turbulence, which is likely to affect the stability of measurement accuracy.

The paper is divided into the following sections. In Section 2, the principle of flow measurement using an orifice is presented, along with the descriptions of the orifices tested and the methodologies for determining the expanded uncertainty of mass flow measurement. Section 3 presents the adopted assumptions and conditions for conducting simulation and experimental tests (for both the centric and eccentric orifice) and the results obtained from these tests. Based on these results, Section 4 discusses the uncertainty of mass flow rate measurement obtained from simulation and experimental tests for the two orifices tested in the assumed range of Reynolds numbers. Final conclusions on the impact of different *Re* values on the uncertainty of mass flow measurement for the tested orifices are given in Section 5.

2. The study

The principle of measuring the flow stream by the means of an orifice is shown in Fig. 1. The most important element of the measuring system is the orifice (2), being a thin disc mounted in a pipe (1) in such a way that the axis of the bore coincides with that of the tube. The fluid dV_1 initially flowing with velocity υ_1 and mass flow rate q_{m1} changes its velocity to υ_2 and the diameter of the cross-section d' as a result of displacement through the orifice (1) with hole diameter d. The result is that different kinetic pressures are upstream of the orifice (p_1) and behind the obstacle (p_2). These pressures are measured using parathyroid pressure gauges (3) and (4). The pressure transducer (5) passes the recorded signals for data acquisition. According to the law of continuity, the flow volumes (dV_1, dV_2) and the mass flow rates (q_{m1}, q_{m2}) of the fluid upstream and downstream of the orifice are equal. The flow continuity is preserved and the fluid density does not change when the fluid flows through different cross sections. Further analysis is based on these assumptions.

Mass flow rate q_m was determined from the formula [15]:

$$q_m = \frac{C \cdot d^2 \cdot \varepsilon \cdot \pi \cdot \sqrt{2 \cdot \Delta p \cdot \rho}}{4 \cdot \sqrt{1 - \left(\frac{d}{D}\right)^4}} \tag{1}$$

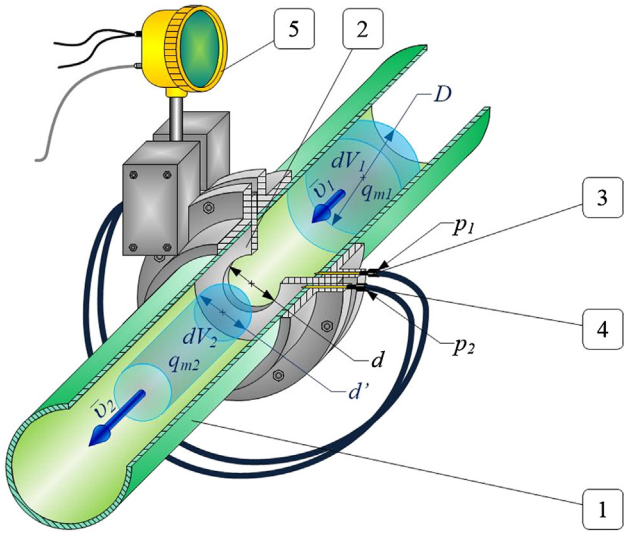

Fig. 1. The measurement principle: 1 – pipe, 2 – orifice, 3, 4 – pressure gauges, 5 – pressure transmitter.

where: C – discharge coefficient [–], d – orifice diameter [m], D – pipe diameter [m], ε - compressibility of a given fluid (for water $\varepsilon = 1$), Δp – differential pressure [Pa], ρ – medium density [kg/m^3].

Analyzed the value of mass flow rate q_m is a function of five parameters (C, d, D, Δp, ρ) of the Eq. (1).

Presented in the article flow measurement uncertainty analysis was carried out considering the following premises:

- the compressibility, velocity and density of the analyzed fluid do not change,
- fluid without internal friction is considered,
- mass flow rate q_m was calculated from $n = 30$ observations.

The aim of the study was to ascertain the measurand estimator of the measured mass flow rate q_m (as the average, in accordance with GUM recommendations [22]) and the expanded uncertainty $U(q_m)$. Assuming the coverage factor $k_p = 2.00$ (which approximately corresponds to the 95% probability of extension), the expanded uncertainty $U(q_m)$ can be determined from the formula [22]:

$$U(q_m) = k_p \cdot u_c(q_m) \tag{2}$$

Complex uncertainty $u_c(q_m)$ is defined as follows [15] (assuming no correlation between the uncertainties of the measured quantities, according to the law of uncertainty propagation [22,23]):

$$u_c(q_m) = \sqrt{u_A^2(q_m) + u_B^2(q_m)} = \sqrt{\begin{array}{c} u_A^2(q_m) + \left(\frac{\partial q_m}{\partial C}\right)^2 \cdot u^2(C) + \left(\frac{\partial q_m}{\partial d}\right)^2 \cdot u^2(d) \\ + \left(\frac{\partial q_m}{\partial D}\right)^2 \cdot u^2(D) + \left(\frac{\partial q_m}{\partial \Delta p}\right)^2 \cdot u^2(\Delta p) \\ + \left(\frac{\partial q_m}{\partial \rho}\right)^2 \cdot u^2(\rho) \end{array}} \tag{3}$$

where $u_A(q_m)$ is the Type A uncertainty [22], $u_B(q_m)$ is the Type B uncertainty [12], and $\frac{\partial q_m}{\partial C}, \frac{\partial q_m}{\partial d}, \frac{\partial q_m}{\partial D}, \frac{\partial q_m}{\partial \Delta p}, \frac{\partial q_m}{\partial \rho}$ are the partial derivates, being the variances of: $u^2(C)$, $u^2(d)$, $u^2(D)$, $u^2(\Delta p)$, and $u^2(\rho)$.

Starting from Eq. (3), after removing the first component regarding uncertainty of type A and transformations, the Eq. (A2) for calculation of relative standard uncertainty of mass flow rate measurement $u(q_m)/q_m$ given in International Standard EN ISO 5167-1: 2003 [27] can be obtained. Engineering calculations according to this standard are presented in the Appendix.

The simulation and experimental investigations of the orifices were performed for the following data: pipe diameter $D = 0.05$ m, compressibility $\varepsilon = 1$.

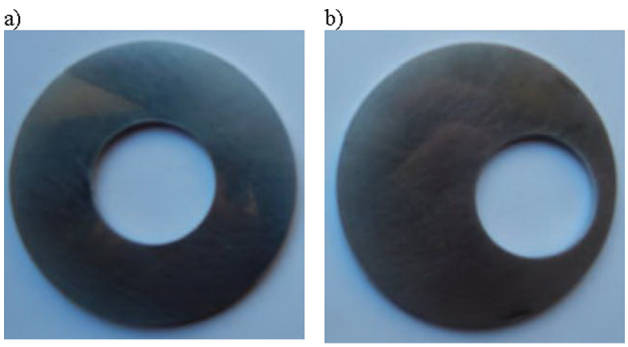

Fig. 2. Photos of tested orifices: a) centric and b) eccentric.

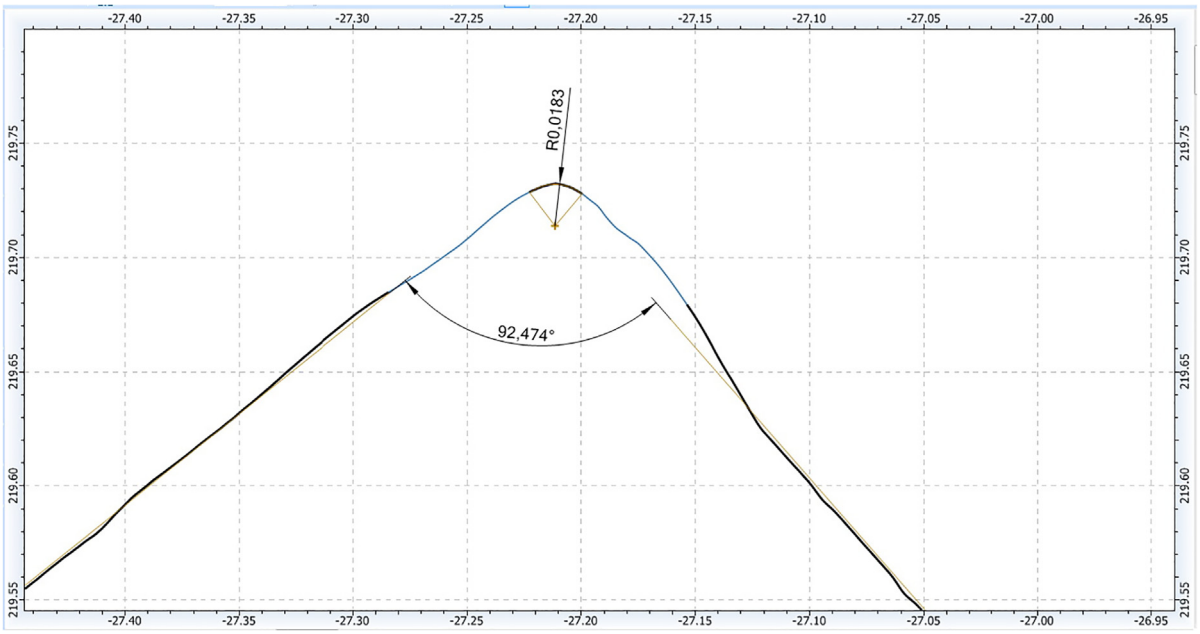

Fig. 3. The result of measuring the inlet edge geometry of the centric orifice (screenshot from software).

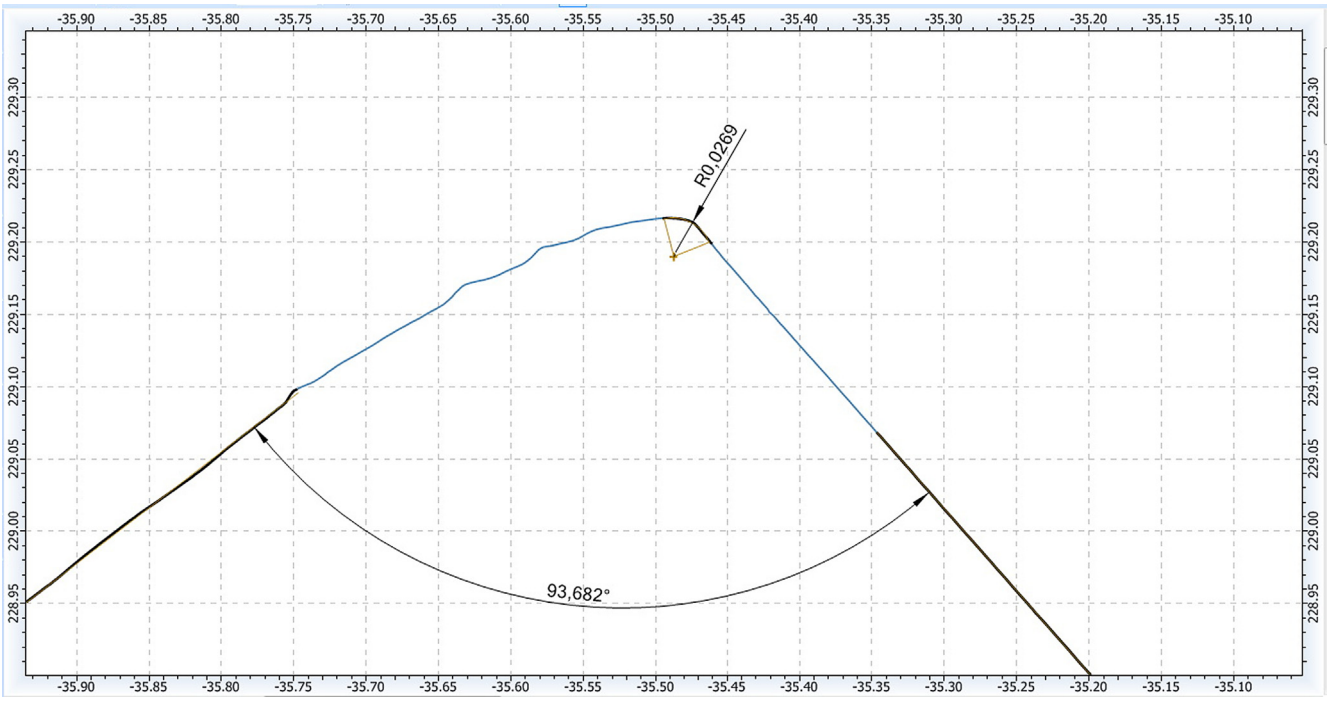

Fig. 4. The result of measuring the inlet edge geometry of the eccentric orifice (screenshot from software).

2.1. Tested orifices

A centric orifice (Fig. 2a) and an eccentric orifice (Fig. 2b) with inner diameters d of 25.005 mm and 24.967 mm, respectively, were selected for the study. The difference in orifice diameters results from the tolerance of their performance, nevertheless the diameter ratio $\beta = d/D$ for both orifices tested has the same value equal to 0.5. Fig. 2 presents the photos of the tested orifices.

The inlet edge geometry of the centric and eccentric orifice was measured on a Wenzel LH 65 coordinate measuring machine (for which the measurement uncertainty is equal to 2.5 μm) in two XY axes. The results of these measurements are presented in graphic form in Figs. 3 and 4 showing the inlet angle and its rounding radius (screenshots from the machine program screen, where R0 is the intake edge radius).

For testing purposes, the eccentric flange was mounted in the housing in such a way that the orifice hole was tangent to the internal diameter of the pipeline, and the accumulation pressure intake holes were located on the opposite side of the contact point. Parietal impulse openings, located in the lower part of the pipeline, were located on a plane passing through the axis of symmetry of the orifice and the axis of symmetry of the pipeline. This plane is

Table 1
Values of absolute errors Δ_g.

Variance	Unit	Δ_g	Distribution
$u^2(d)$	[m^2]	0.01 mm	Rectangular
$u^2(D)$	[m^2]	0.01 mm	
$u^2(\Delta p)$	[Pa^2]	3.6 Pa	
$u^2(\rho)$	$\left[\frac{kg^2}{m^6}\right]$	0.5 kg/m^3	

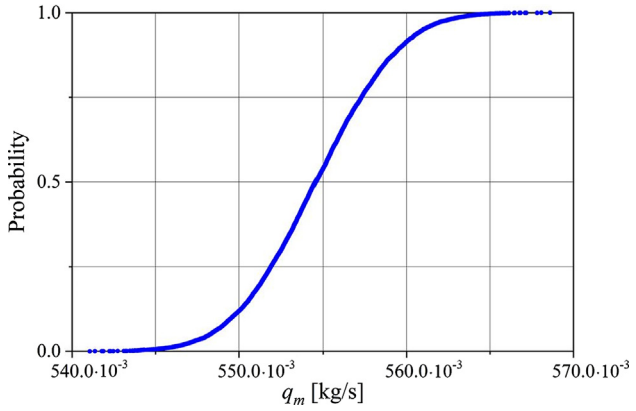

Fig. 5. Generated flow distribution for q_m = 554.6 · 10^{-3} $\frac{kg}{s}$ centric orifice.

deviated from the vertical diameter of the pipeline by an angle of 45°. For measurement purposes, the parathyroid impulse holes were placed at the same height, identically for the eccentric or centric orifice.

Studies were performed for these two orifices for Reynolds numbers in the range 10,000 ≤ *Re* ≤ 20,000 and temperature *T* in the range (291.15 … 301.65) K (for all measurement series performed for all tested flows). In each one measurement series (for each mass flow tested) consisting of 30 tests, the temperature change did not exceed 2 K.

3. Research results

This section presents the results of the simulation and experimental research for the centric and eccentric orifice.

3.1. Simulations

The simulations of the mass flow rate uncertainty estimation were made using the Monte Carlo (MC) numerical method [26,29].

This method is used to check uncertainty results obtained from analytical calculations. Often this method is used when the measurement method is an indirect method and also when the measurement function is not linear.

Detailed stages of this method are described in [12].

It is assumed that the measured mass flow rate q_m is given by the following equation:

$$q_m = \overline{q_m} + c_0 \cdot u_A(q_m) + c_1 \cdot u(C) + c_2 \cdot u(d) + c_3 \cdot u(D) + c_4 \cdot u(\Delta p) + c_5 \cdot u(\rho) \quad (4)$$

where: $\overline{q_m}$ is the arithmetic average of n observation of flows, and c_0 to c_5 represent the sensitivity coefficients - corresponding partial derivatives.

Table 1 presents the adopted probability distributions, and the value of absolute errors to the examined parameters (based on the accuracy of their measurement).

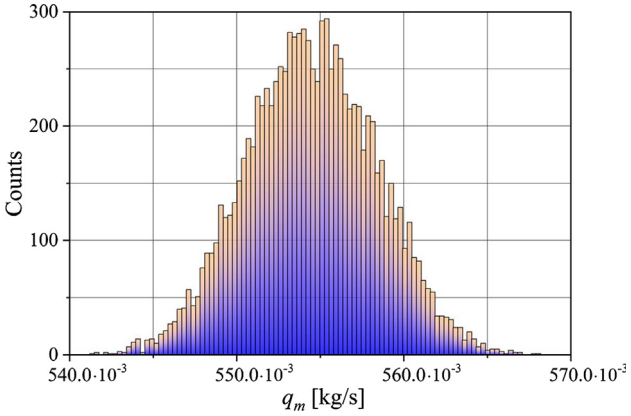

Fig. 6. Histogram of generated values of mass flow rate - centric orifice.

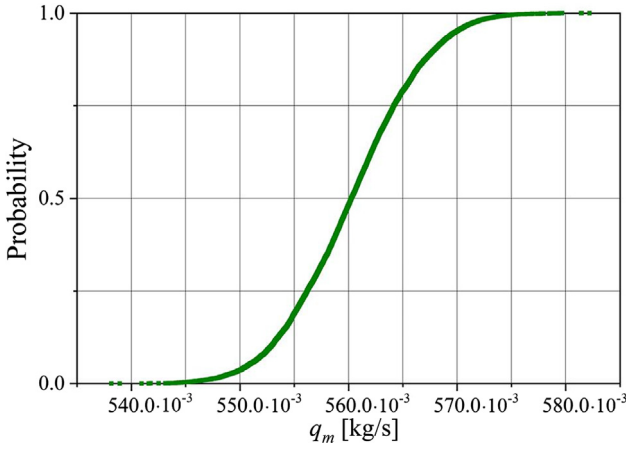

Fig. 7. Generated flow distribution for q_m = 560.3 · 10^{-3} $\frac{kg}{s}$ eccentric orifice.

The relative uncertainty of the coefficient *C* was calculated in accordance with the recommendations of the standard EN ISO 5167-2: 2003 [28]:

$$\frac{u(C)}{C} = 0.5 + 0.9 \cdot (0.75 - \beta) \cdot \left(2.8 - \frac{D}{25,4}\right) = 0.5 + 0.9 \cdot (0.75 - 0.5) \cdot \left(2.8 - \frac{50}{25.4}\right) = 0.687\% \quad (5)$$

For the analyzed data, uncertainty estimates were carried out in Microsoft Excel for six different mass flow rates q_m using the MC method (the number of samples *M* was equal to 10^4).

Fig. 5 shows a generated probability density function (PDF) of the simulated numerical values of the mass flow rate q_m = 554.6 · 10^{-3} $\frac{kg}{s}$ for centric orifice.

Based on these results, a histogram with the width of intervals of 0.4 · 10^{-3} $\frac{kg}{s}$ was prepared (Fig. 6).

Fig. 7 presents a generated PDF for q_m = 560.3 · 10^{-3} $\frac{kg}{s}$ for eccentric orifice.

A histogram for the above data is presented in Fig. 8 (with the width of intervals of 0.4 · 10^{-3} $\frac{kg}{s}$).

The results of estimating $U(q_m)$ of the mass flow rate with the measurand q_m are summarized in Table 2 for all measuring points. This table also presents relative uncertainty values $\delta U(q_m)$ determined from the relationship:

$$\delta U(q_m) = \frac{U(q_m)}{q_m} \cdot 100\% \quad (6)$$

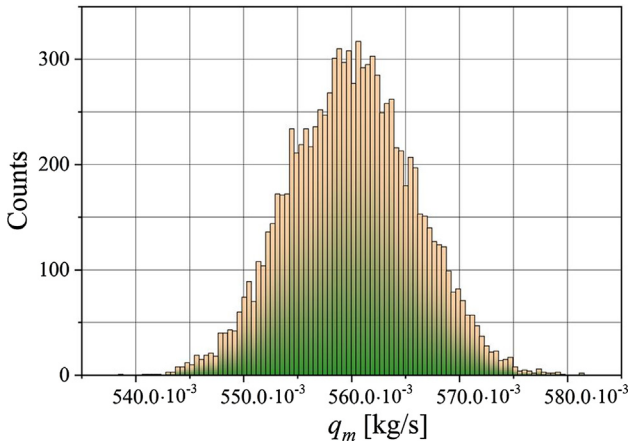

Fig. 8. Histogram of generated values of mass flow rate - eccentric orifice.

The Reynolds number *Re* was estimated from the equation:

$$Re = \frac{4 \cdot q_m}{\pi \cdot D \cdot \eta} \tag{7}$$

where η is the dynamic viscosity [Pa·s].

The simulation results obtained from the MC method have revealed that in the analyzed range of Reynolds numbers the expanded uncertainty $U(q_m)$ does not exceed $12.7 \cdot 10^{-3}\ \frac{kg}{s}$.

For the centric orifice, the lowest uncertainty value $U(q_m) = 5.5 \cdot 10^{-3}\ \frac{kg}{s}$ was obtained for $q_m = 398.6 \cdot 10^{-3}\ \frac{kg}{s}$, while the largest $U(q_m) = 8.7 \cdot 10^{-3}\ \frac{kg}{s}$ for the mass flow rate equal to $639.9 \cdot 10^{-3}\ \frac{kg}{s}$.

For the eccentric orifice, the obtained uncertainty results are similar for each flow value. The largest uncertainty value is equal to $12.6 \cdot 10^{-3}\ \frac{kg}{s}$ and occurs for the mass flow rate $630.6 \cdot 10^{-3}\ \frac{kg}{s}$.

3.2. Experiments

Experiments with the orifices tested were carried out on the stand presented in Fig. 9.

In the experimental research installation the water flow was imposed by a centrifugal pump in a closed system. Flow through the vent responsible for removing air bubbles from the fluid. Regulation of the flow of water in the installation carried out the valve with exchangeable bleed. The major part of the water flow passed through a measuring pipe made of stainless steel. A standard orifice with diameter ratio $\beta = 0.5$ was installed in the pipe with inner diameter of $D = 50$ mm.

The difference of static pressures in front of and behind the orifice was measured with a programmed differential pressure transmitter APR 2000/ALW, with the measuring range equals 2.4 kPa. The relative error of this transmitter is 0.15% of the base. A view of this transmitter on the laboratory stand is shown in Fig. 10. In the tested system, the electromagnetic flowmeter type PROMAG 30AT15 is the reference flow meter. The maximum permissible

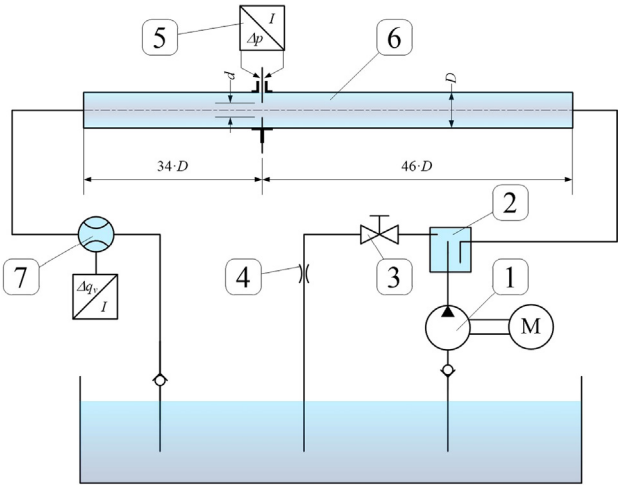

Fig. 9. Experimental research installation [15]: 1 – centrifugal pump, 2 – vent, 3 – valve, 4 – exchangeable bleed, 5 – differential pressure transmitter, 6 – pipe, 7 – electromagnetic flowmeter.

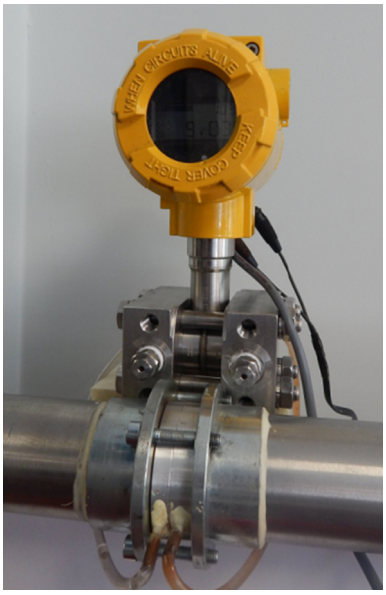

Fig. 10. APR-2000/ALW transducer mounted on the laboratory stand.

error of this instrument is $\Delta q_v = 0.0092\ dm^3/s$ (in the tested measuring range).

The same data values were used to conduct experimental studies. For each of the 6 flows, 30 measurements were taken at the laboratory stand shown schematically in Fig. 9. The remaining part of this section presents the results obtained experimentally for the

Table 2
Measurand values and uncertainty from MC method.

Centric orifice				Eccentric orifice			
Re	$q_m \cdot 10^{-3}\ \left[\frac{kg}{s}\right]$	$U(q_m) \cdot 10^{-3}\ \left[\frac{kg}{s}\right]$	$\delta\ U(q_m)$ [%]	*Re*	$q_m \cdot 10^{-3}\ \left[\frac{kg}{s}\right]$	$U(q_m) \cdot 10^{-3}\ \left[\frac{kg}{s}\right]$	$\delta\ U(q_m)$ [%]
11,688	398.6	5.5	1.38	11,715	457.9	9.0	1.98
13,957	466.5	6.4	1.38	13,338	529.3	10.4	1.96
14,872	500.4	6.8	1.36	13,783	560.3	11.3	2.02
16,766	554.6	7.6	1.36	15,176	593.2	11.5	1.94
18,077	587.7	7.9	1.35	15,579	630.6	12.6	2.00
19,840	639.9	8.7	1.36	16,730	636.7	12.2	1.92

Table 3
Results of mass flow rate for centric orifice.

Sample No	$q_m \cdot 10^{-3}$ $\left[\frac{kg}{s}\right]$	Sample No	$q_m \cdot 10^{-3}$ $\left[\frac{kg}{s}\right]$	Sample No	$q_m \cdot 10^{-3}$ $\left[\frac{kg}{s}\right]$
1.	554.9	11.	554.5	21.	554.4
2.	555.2	12.	555.0	22.	555.4
3.	555.2	13.	555.0	23.	555.5
4.	554.9	14.	555.2	24.	553.6
5.	555.1	15.	554.7	25.	553.9
6.	554.9	16.	555.2	26.	553.6
7.	554.5	17.	555.0	27.	553.3
8.	555.0	18.	554.9	28.	553.1
9.	554.7	19.	554.6	29.	553.2
10.	553.9	20.	554.8	30.	553.4

Table 4
Results of mass flow rate q_m for eccentric orifice.

Sample No	$q_m \cdot 10^{-3}$ $\left[\frac{kg}{s}\right]$	Sample No	$q_m \cdot 10^{-3}$ $\left[\frac{kg}{s}\right]$	Sample No	$q_m \cdot 10^{-3}$ $\left[\frac{kg}{s}\right]$
1.	560.5	11.	561.3	21.	561.4
2.	560.0	12.	561.0	22.	560.1
3.	559.8	13.	561.3	23.	559.7
4.	557.3	14.	561.4	24.	559.4
5.	559.9	15.	561.8	25.	559.0
6.	560.1	16.	560.6	26.	559.1
7.	561.0	17.	559.7	27.	559.1
8.	561.2	18.	561.2	28.	559.1
9.	561.0	19.	561.2	29.	559.3
10.	561.0	20.	561.5	30.	560.0

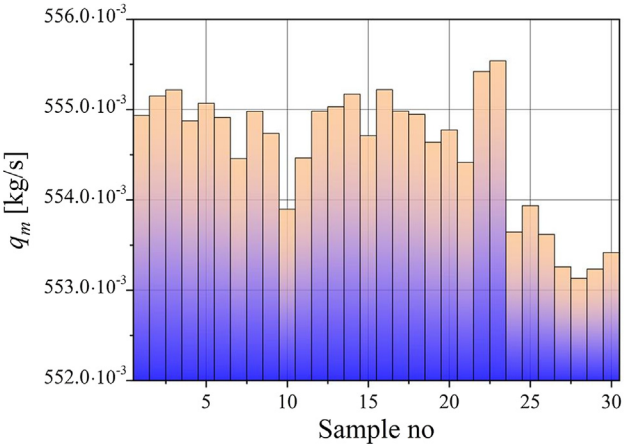

Fig. 11. Measured mass flow rate q_m for centric orifice.

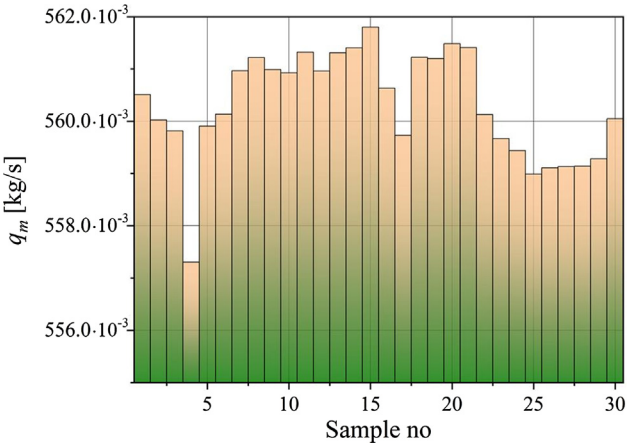

Fig. 12. Measured mass flow rate q_m for eccentric orifice.

two tested orifices, for the similar mass flow rate approximately equal to $550.0 \cdot 10^{-3}\ \frac{kg}{s}$.

Tables 3 and 4 summarize the results from the experiment for the centric and eccentric orifice, respectively.

Figs. 11 and 12 present graphically the data from Tables 3 and 4 as function of the measurement number.

Table 5 summarizes the estimates of the mass flow rate q_m and the uncertainty of its measurement obtained on the basis of data for all flows through the centric and eccentric orifice.

On the basis of the obtained results, it can be concluded that the smallest $U(q_m)$ value was obtained for q_m equals $398.6 \cdot 10^{-3}\ \frac{kg}{s}$ for centric orifice, and for $q_m = 457.9 \cdot 10^{-3}\ \frac{kg}{s}$ for eccentric orifice. The largest values of the expanded uncertainty were obtained for: the largest mass flow rate q_m equals $639.9 \cdot 10^{-3}\ \frac{kg}{s}$ for the centric orifice, and for q_m equals $630.6 \cdot 10^{-3}\ \frac{kg}{s}$ for the eccentric orifice. For the centric orifice, the uncertainty results obtained are smaller almost for each flow.

4. Discussion

The flow tests were carried out on the laboratory stand shown in Fig. 9. During the tests, such parameters as: accumulation pressure at the tested orifice, temperature of the flowing water, and flow volume, were measured and recorded using the PC LINK Plus computer measuring system.

Based on the obtained experimental results, the values of the flow constant C for the centric and eccentric orifice for Reynolds numbers in the range $10{,}000 \leq Re \leq 20{,}000$ were determined. The obtained values confirm the correctness of the adopted measurement methodology (Fig. 13).

Table 5
Results of the measured mass flow rate q_m and the uncertainty obtained from experiment.

Centric orifice				Eccentric orifice			
Re	$q_m \cdot 10^{-3}$ $\left[\frac{kg}{s}\right]$	$U(q_m) \cdot 10^{-3}$ $\left[\frac{kg}{s}\right]$	$\delta\, U(q_m)$[%]	*Re*	$q_m \cdot 10^{-3}$ $\left[\frac{kg}{s}\right]$	$U(q_m) \cdot 10^{-3}$ $\left[\frac{kg}{s}\right]$	$\delta\, U(q_m)$[%]
11,688	398.6	5.6	1.41	11,715	457.9	9.2	2.02
13,957	466.4	6.5	1.40	13,338	529.3	10.7	2.03
14,872	500.4	7.0	1.40	13,783	560.3	11.6	2.07
16,766	554.6	7.7	1.39	15,176	593.2	11.9	2.01
18,077	587.7	8.2	1.39	15,579	630.6	13.0	2.07
19,840	639.9	8.9	1.39	16,730	636.7	12.7	1.99

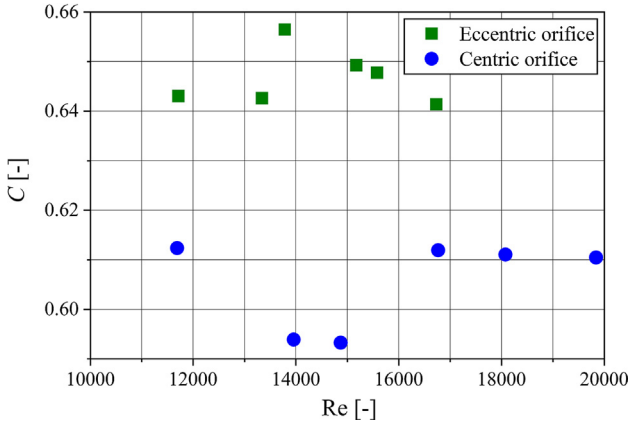

Fig. 13. Values of flow constant C obtained for centric and eccentric orifice.

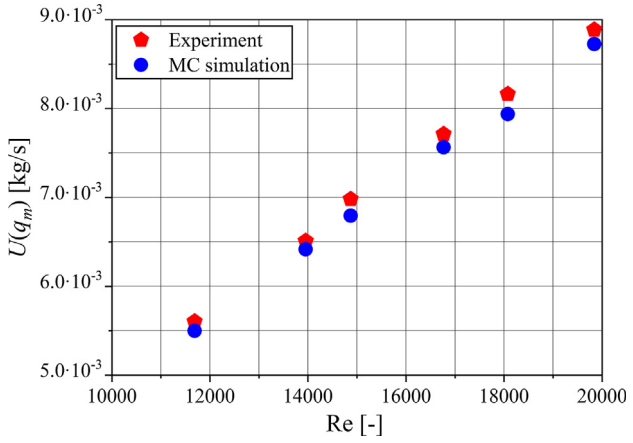

Fig. 14. Comparison of expanded uncertainties $U(q_m)$ from simulation and experiment for centric orifice.

As described in Section 3.1, the two orifices were also subjected to simulation tests (with diameter ratio $\beta = 0.5$) under comparable conditions. After comparing the experimental and simulation tests, it turned out that different results of expanded uncertainty of flow measurement were obtained for various Reynolds numbers in the range $10{,}000 \leq Re \leq 20{,}000$.

Figs. 14 and 15 show the uncertainties $U(q_m)$ obtained from the MC method and from experiment for the centric and eccentric orifice, respectively.

The results obtained for the centric and eccentric orifice have shown that for both orifice types the results acquired from the experiment and from MC simulation are similar. Larger discrepancies between the results from simulation and experiment were found for the eccentric orifice. For similar flow streams for the

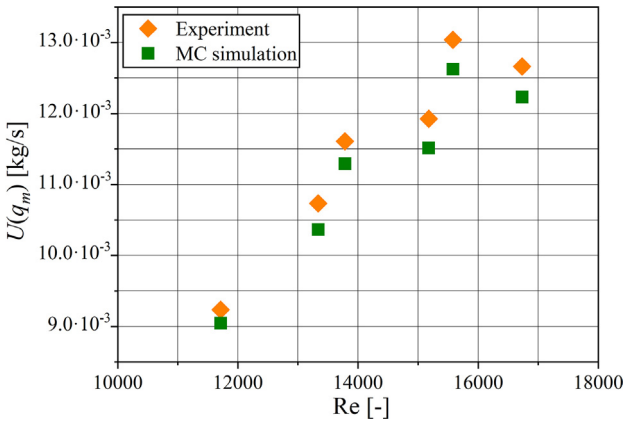

Fig. 15. Comparison of expanded uncertainties $U(q_m)$ from simulation and experiment for eccentric orifice.

eccentric orifice, higher values of stream measurement uncertainty were obtained, for which part of the flow is a boundary layer due to the point of contact of the orifice hole with the internal diameter of the pipeline. In these conditions, an asymmetrical distribution of the velocity profile in the longitudinal section behind the orifice is created.

The nature of changes in the expanded uncertainty $U(q_m)$ of the flow measurement for each orifice is the same. For both orifices, the value of $U(q_m)$ increases in the studied range of Reynolds number changes.

5. Conclusion

The article presents the results of estimating the expanded uncertainty $U(q_m)$ of mass flow rate measurement, obtained from the Monte Carlo simulation and experimental tests. The object of the research were two measuring orifices: centric and eccentric. The aim of the study was to examine whether changes in the nature of the flow rate measurement uncertainty depend on the type of installation flanges when the Reynolds number changes in the range $10{,}000 \leq Re \leq 20{,}000$.

Based on the obtained experimental results, it was found that the value of the expanded uncertainty $U(q_m)$ changes with the increase in the Reynolds number irrespective of the type of the orifice used. In the studied range of Reynolds numbers, the values of estimated uncertainty $U(q_m)$ were in the range of $12.7 \cdot 10^{-3}$ $\frac{kg}{s}$. In the studied range of Reynolds numbers, the estimated uncertainty values $U(q_m)$ were similar. For comparison, the Monte Carlo simulation for centric orifice and flow $q_m = 398.6 \cdot 10^{-3}$ $\frac{kg}{s}$ gave $U(q_m) = 5.5 \cdot 10^{-3}$ $\frac{kg}{s}$, while for eccentric orifice and flow $q_m = 457.9 \cdot 10^{-3}$ $\frac{kg}{s}$ the uncertainty $U(q_m)$ was $9.0 \cdot 10^{-3}$ $\frac{kg}{s}$.

Moreover, for the eccentric orifice, the obtained estimated uncertainty results were higher almost for each flow value, and

the largest difference, amounting to $0.5 \cdot 10^{-3}\ \frac{kg}{s}$ was recorded for the largest mass flow rates, for $q_m = 636.7 \cdot 10^{-3}\ \frac{kg}{s}$.

It is noteworthy that the obtained measurement results confirmed the same nature of flow measurement uncertainty changes in different orifice types. For the both orifices types, the nature of these changes can be estimated as linear - as the flow increases, the value of the expanded uncertainty $U(q_m)$ of the flow measurement also increases.

The presented results of the analysis of the relative uncertainty $\delta U(q_m)$ of water flow rate measurement (obtained from both: the Monte Carlo simulation and the experiment) indicate that in the considered Reynolds numbers range $10{,}000 \leq Re \leq 20{,}000$, the values of this uncertainty are relatively constant. For the centric orifice the value of $\delta U(q_m)$ does not exceed 1.42%, and for eccentric orifice $\delta U(q_m)$ does not exceed 2.08%. Very similar results were obtained for engineering calculations according to the EN ISO 5167-1: 2003 standard presented in the Appendix: $\delta U(q_m)$ = 1.38% for centric orifice, and $\delta U(q_m)$ = 2.00% for eccentric orifice respectively.

The authors intend to make a mathematical model of orifice flow based on the collected experimental data.

This will allow to include of a larger number of possible flow cases, and thus for consideration of other phenomena that influence to estimate flow measurement uncertainty. In addition, based on simulations it would be possible to optimize the measurement process. This type of approach is recognized as a way of analyzing complex forms of liquid transport, e.g. in porous media, as described in the articles [30–32].

CRediT authorship contribution statement

Anna Golijanek-Jędrzejczyk: Conceptualization, Methodology, Software, Formal analysis, Writing - original draft. **Andrzej Mrowiec:** Investigation, Resources, Validation, Writing - review & editing. **Robert Hanus:** Validation, Writing - review & editing. **Marcin Zych:** Visualization, Validation, Writing - review & editing. **Dariusz Świsulski:** Writing - review & editing.

Declaration of Competing Interest

The authors declare that they have no known competing financial interests or personal relationships that could have appeared to influence the work reported in this paper.

Acknowledgements

This publication is partially supported by AGH University of Science and Technology (project number 16.16.140.315), by Rzeszów University of Technology (project number DS. EM.18.001), and by Polish Ministry of Science and Higher Education under the program "Regional Initiative of Excellence" in 2019 – 2022. Project number 027/RID/2018/19, funding amount 11 999 900 PLN.

Appendix

In engineering practice, mass flow rate uncertainty calculations based on EN ISO 5167-1: 2003 [27] are used. The calculations of the relative values of expanded uncertainty $U(q_m)/q_m$ for mass flow rate measurement q_m, for the centric and eccentric orifice are presented below. As in the manuscript, the following data were adopted:

C = 0.6105
D = 0.05 m
d = 0.025 m
Δp = 2147.6 kPa
ρ = 1000 kg/m^3
β = 0.5

The relative value of the expanded uncertainty $U(q_m)/q_m$ of measurement of mass flow rate q_m is defined as:

$$\frac{U(q_m)}{q_m} = \frac{k_p \cdot u(q_m)}{q_m} \tag{A1}$$

where: k_p = 2.0.

The relative complex standard uncertainty $u(q_m)/q_m$ of mass flow rate measurement q_m according to EN ISO 5167-1: 2003 standard can be calculated from the following relationship:

$$\frac{u(q_m)}{q_m} = \sqrt{\left(\frac{u(C)}{C}\right)^2 + \left(\frac{2\cdot\beta^4}{1-\beta^4}\right)^2 \cdot \left(\frac{u(D)}{D}\right)^2 + \left(\frac{2}{1-\beta^4}\right)^2 \cdot \left(\frac{u(d)}{d}\right)^2 + \frac{1}{4}\cdot\left(\frac{u(\Delta p)}{\Delta p}\right)^2 + \frac{1}{4}\cdot\left(\frac{u(\rho)}{\rho}\right)^2} \tag{A2}$$

The values of relative uncertainty of individual parameters were adopted the same as in the article. The relative uncertainty of the C coefficient is calculated from the formula:

$$\frac{u(C)}{C} = 0.5 + 0.9\cdot(0.75-\beta)\cdot\left(2.8 - \frac{D}{25{,}4}\right) = 0.5 + 0.9\cdot(0.75-0.5)\cdot\left(2.8-\frac{50}{25.4}\right) = 0.687\% \tag{A3}$$

Then the relative uncertainty of pipeline diameter D is determined using equation (where Δ_{gD} is absolute pipe diameter D error):

$$\frac{u(D)}{D} = \frac{\Delta_{gD}\cdot 100\%}{D\cdot\sqrt{3}} = \frac{0.01\ \text{mm}\cdot 100\%}{50\ \text{mm}\cdot\sqrt{3}} = 0.01\% \tag{A4}$$

and for the diameter d of the orifice (Δgd is absolute orifice diameter d error):

$$\frac{u(d)}{d} = \frac{\Delta_{gd}\cdot 100\%}{d\cdot\sqrt{3}} = \frac{0.01\ \text{mm}\cdot 100\%}{25\ \text{mm}\cdot\sqrt{3}} = 0.02\% \tag{A5}$$

The next step is to calculate the relative uncertainties for measuring the pressure difference Δp and density ρ, as follows:

$$\frac{u(\Delta p)}{\Delta p} = \frac{\sqrt{\left(\frac{\Delta_g\cdot\Delta p_{range}}{\sqrt{3}}\right)^2}}{\Delta p}\cdot 100\% = \frac{\sqrt{\left(\frac{0.01\frac{1}{\%}\cdot 0.15\%\cdot 2400\ \text{Pa}}{\sqrt{3}}\right)^2}}{2147.6\ \text{Pa}}\cdot 100\% = 0.097\% \tag{A6}$$

$$\frac{u(\rho)}{\rho} = \frac{0.5\ \frac{\text{kg}}{\text{m}^3}\cdot 100\%}{1000\ \frac{\text{kg}}{\text{m}^3}} = 0.05\% \tag{A7}$$

It was assumed that the temperature changes in one measurement series do not exceed 2 K. Then the relative standard uncertainty of mass flow rate measurement $u(q_m)/q_m$ for the centric orifice is:

$$\frac{u(q_m)}{q_m} = \sqrt{0.687^2 + 0.0178 \cdot 0.01^2 + 4.55 \cdot 0.02^2 + 0.25 \cdot 0.097^2 + 0.25 \cdot 0.05^2} = 0.69\% \quad \text{(A8)}$$

and the relative expanded uncertainty of mass flow rate measurement $U(q_m)/q_m$ for the centric orifice is equal:

$$\frac{U(q_m)}{q_m} = \frac{k_p \cdot u(q_m)}{q_m} = 1.38\% \quad \text{(A9)}$$

The relative standard uncertainty of mass flow rate measurement $u(q_m)/q_m$ for the eccentric orifice has been determined analogously to the uncertainty for centric orifice (only the relative uncertainty of the C coefficient is different, which is 1% for the eccentric orifice according to the report ISO / TR 15377: 1998 as amended AC1 from 1999.):

$$\frac{u(q_m)}{q_m} = \sqrt{1.0^2 + 0.0178 \cdot 0.01^2 + 4.55 \cdot 0.02^2 + 0.25 \cdot 0.097^2 + 0.25 \cdot 0.05^2} = 1.002\% \quad \text{(A10)}$$

Then the relative expanded uncertainty of mass flow rate measurement $U(q_m)/q_m$ for the eccentric orifice is:

$$\frac{U(q_m)}{q_m} = \frac{k_p \cdot u(q_m)}{q_m} = 2.004\% \quad \text{(A11)}$$

References

[1] M. Moosa, M.H. Hekmat, Numerical investigation of turbulence characteristics and upstream disturbance of flow through standard and multi-hole orifice flowmeters, Flow Meas. Instrum. 65 (2019) 203–218, https://doi.org/10.1016/j.flowmeasinst.2019.01.002.

[2] J. Dong et al., Study on the measurement accuracy of an improved cemented carbide orifice flowmeter in natural gas pipeline, Flow Meas. Instrum. 99 (2018) 52–62, https://doi.org/10.1016/j.flowmeasinst.2017.12.008.

[3] J.A. Fedchak, D.R. Defibaugh, Accurate conductance measurements of a pinhole orifice using a constant-pressure flowmeter, Measurement 45 (10) (2012) 2449–2451, https://doi.org/10.1016/j.measurement.2011.10.046.

[4] A. Bekraoui, A. Hadjadj, A. Benmounah, M. Oulhadj, Uncertainty study of fiscal orifice meter used in a gas Algerian field, Flow Meas. Instrum. 66 (2019) 200–208, https://doi.org/10.1016/j.flowmeasinst.2019.01.020.

[5] M.R. Rzasa, B. Tomaszewska-Wach, Measurement of the wet gas stream with a standard orifice, Przegl. Elektrotech. 95 (11) (2019) 86–89, https://doi.org/10.15199/48.2019.11.23 (in Polish).

[6] H.M. Abd, O.R. Alomar, I.A. Mohamed, Effects of varying orifice diameter and Reynolds number on discharge coefficient and wall pressure, Flow Meas. Instrum. 65 (2019) 219–226, https://doi.org/10.1016/j.flowmeasinst.2019.01.004.

[7] G. Falcone, G.F. Hewitt, C. Alimonti, Multiphase Flow Metering: Principles and Applications, Elsevier, Amsterdam, 2009.

[8] R. Thorn, G.A. Johansen, B.T. Hjertaker, Three-phase flow measurement in the petroleum industry, Meas. Sci. Technol. 24 (2013), https://doi.org/10.1088/0957-0233/24/1/012003.

[9] S. Pirouzpanah, M. Çevik, G.L. Morrison, Multiphase flow measurements using coupled slotted orifice plate and swirl flow meter, Flow Meas. Instrum. 40 (2014) 157–161, https://doi.org/10.1016/j.flowmeasinst.2014.09.005.

[10] G.H. Roshani, E. Nazemi, A high performance gas–liquid two-phase flow meter based on gamma-ray attenuation and scattering, Nucl. Sci. Tech. 28 (11) (2017) 169, https://doi.org/10.1007/s41365-017-0310-z.

[11] P. Piechota, P. Synowiec, A. Andruszkiewicz, W. Wędrychowicz, Selection of the relevant turbulence model in a CFD Simulation of a flow disturbed by hydraulic elbow - comparative analysis of the simulation with measurements results obtained by the ultrasonic flowmeter, J. Therm. Sci. 27 (5) (2018) 413–420, https://doi.org/10.1007/s11630-018-1034-z.

[12] A. Golijanek-Jędrzejczyk, D. Świsulski, R. Hanus, M. Zych, L. Petryka, Uncertainty of the liquid mass flow measurement using the orifice plate, Flow Meas. Instrum. 62 (2018) 84–92, https://doi.org/10.1016/j.flowmeasinst.2018.05.012.

[13] C.R. Samples, Orifice flow measurement uncertainty, Proc. Int. Sch. Hydrocarb. Meas. (1984) 161–165.

[14] H. Yoshida, M. Shiro, K. Arai, H. Akimichi, M. Hirata, Calculation and uncertainty evaluation of conductance of a precise orifice for orifice-flow method, Vacuum 84 (2009) 277–279, https://doi.org/10.1016/j.vacuum.2009.04.033.

[15] A. Golijanek-Jędrzejczyk, A. Mrowiec, R. Hanus, M. Zych, D. Świsulski, Determination of the uncertainty of mass flow measurement using the orifice for different values of the Reynolds number, EPJ WoC 213 (2019) 02022, https://doi.org/10.1051/epjconf/201921302022.

[16] Y.Q. Xu, Y. Peet, D. Coxe, T. Lee, Computational modeling of flow rate measurements using an orifice flow meter, in: Development and Applications in Computational Fluid Dynamics; Industrial and Environmental Applications of Fluid Mechanics; Fluid Measurement and Instrumentation; Cavitation and Phase Change. Vol. 2. American Society of Mechanical Engineers (ASME), (2018) Doi: 10.1115/FEDSM2018-83296.

[17] U. Otgonbaatar, E. Baglietto, N. Todreas, Methodology for characterizing representativeness uncertainty in orifice plate mass flow rate measurements using CFD simulations, Nucl. Sci. Eng. 184 (3) (2016) 430–440, https://doi.org/10.13182/NSE16-9.

[18] J. Gao, F. Wu, Investigation of flow through the two-stage orifice, Eng. Appl. Comp. Fluid 13 (1) (2019) 117–127, https://doi.org/10.1080/19942060.2018.1561517.

[19] M. Durdević, M. Bukurov, S. Tašin, S. Bikić, Experimental research of single-hole and multi-hole orifice gas flow meters, Flow Meas. Instrum. 70 (2019), https://doi.org/10.1016/j.flowmeasinst.2019.101650 101650.

[20] N. Furuichi, Y. Terao, S. Ogawa, L. Cordova, T. Shimada, Inter-laboratory comparison of small water flow calibration facilities with extremely low uncertainty, Measurement 91 (2016) 548–556, https://doi.org/10.1016/j.measurement.2016.05.088.

[21] I.I. Shinder, M.R. Moldover, Feasibility of an accurate dynamic standard for water flow, Flow Meas. Instrum. 21 (2) (2010) 128–133, https://doi.org/10.1016/j.flowmeasinst.2010.01.008.

[22] Guide to the Expression of Uncertainty in Measurement, Joint Committee for Guides in Metrology (JCGM) 100:2008.

[23] J. Taylor, Introduction to Error Analysis the Study of Uncertainties in Physical Measurements, 2nd ed., University Science Books, New York, 1997.

[24] S. Chun, B.R. Yoon, H.M. Choi, Uncertainty estimation of a liquid flow standard system with small flow rates, in: 16th International Flow Measurement Conference 2013, FLOMEKO 2013 (2013).

[25] O. Büker, P. Lau, K. Tawackolian, Reynolds number dependence of an orifice plate, Flow Meas. Instrum. 30 (2013) 123–132, https://doi.org/10.1016/j.flowmeasinst.2013.01.009.

[26] G. Raiteri, A. Bordone, T. Ciuffardi, F. Pennecchi, Uncertainty evaluation of CTD measurements: a metrological approach to water-column coastal parameters in the Gulf of La Spezia area, Measurement 126 (2018) 156–163, https://doi.org/10.1016/j.measurement.2018.05.058.

[27] EN ISO 5167-1: 2003 Measurement of fluid flow by means of pressure differential devices inserted in circular cross-section conduits running full - Part 1: General principles and requirements.

[28] EN ISO 5167-2: 2003 Measurement of fluid flow by means of pressure differential devices inserted in circular cross-section conduits running full - Part 2: Orifice plates.

[29] Supplement 1 to the Guide to the expression of uncertainty in measurement – Propagation of distributions using a Monte Carlo method, JCGM 101:2008.

[30] M. Matyka, A. Khalili, Z. Koza, Tortuosity-porosity relation in porous media flow, Phys. Rev. E - Stat. Nonlinear, Soft Matter Phys. 78 (2008), https://doi.org/10.1103/PhysRevE.78.026306 026306.

[31] P. Madejski, P. Krakowska, M. Habrat, E. Puskarczyk, M. Jędrychowski, Comprehensive approach for porous materials analysis using a dedicated preprocessing tool for mass and heat transfer modeling, J. Therm. Sci. 27 (2018) 479–486, https://doi.org/10.1007/s11630-018-1043-y.

[32] P. Krakowska, Detailed parametrization of the pore space in tight clastic rocks from Poland based on laboratory measurement results, Acta Geophys. 67 (2019) 1765–1776, https://doi.org/10.1007/s11600-019-00331-0.